Improvement of the off-state breakdown voltage with field plate and low-density drain in AlGaN/GaN high-electron mobility transistors*

Zhang Peng(张 鹏), Zhao Sheng-Lei(赵胜雷), Hou Bin(侯 斌), Wang Chong(王 冲), Zheng Xue-Feng(郑雪峰), Ma Xiao-Hua(马晓华)†, Zhang Jin-Cheng(张进成), and Hao Yue(郝 跃)

Key Laboratory of Wide Band-Gap Semiconductor Materials and Devices, School of Advanced Materials and Nanotechnology, Xidian University, Xi'an 710071, *China*

(Received 19 June 2014; revised manuscript received 16 September 2014; published online 19 January 2015)

We present an AlGaN/GaN high-electron mobility transistor (HEMT) device with both field plate (FP) and low-density drain (LDD). The LDD is realized by the injection of negatively charged fluorine (F^-) ions under low power in the space between the gate and the drain electrodes. With a small-size FP and a LDD length equal to only 31% of the gate-drain spacing, the device effectively modifies the electric field distribution and achieves a breakdown voltage enhancement up to two times when compared with a device with only FP.

Keywords: GaN, high-electron mobility transistors, fluorine, electric field

PACS: 73.61.Ey, 85.30.Tv, 52.77.Dq **DOI:** 10.1088/1674-1056/24/3/037304

1. Introduction

GaN-based high-electron mobility transistors (HEMTs) are excellent candidates for power electronics applications due to their superior material properties, such as high electron mobility and high energy band gap.[1] The application of GaN HEMTs is limited by the lack of a normally-off device, device cost, and reliability issues, such as current collapse. For many years breakdown character has also been a major concern of GaN device reliability in power electronics applications. The theoretical critical electric-field of GaN is 3.3 MV/cm, which is ten times higher than that of Si material.[2] So the breakdown voltage (BV) of a GaN device is supposed to be very tempting theoretically. However, the actual BV of I-gate (gate without field plate structure) HEMT is usually below 100 V, which is unacceptable in high voltage applications.[3–5] Meanwhile, to compensate for the reduction in the maximum current and to maintain similar power handling capability in enhancement-mode devices, the BV needs to be improved without increasing the gate-to-drain distance because it inevitably increases the device size.[6]

The main reason of the low BV is that the electric field (E-field) is extremely concentrated near the gate edge due to the thin conducting channel in AlGaN/GaN hetero structures. Given that the theoretical critical electric-field of AlGaN is much higher than GaN due to the composition of Al, the GaN buffer near the hetero interface suffers early breakdown. The major solution of the breakdown issue is placing a field-plate (FP) structure above the gate edge, including gate-plate and source-plate. A lot of work has been done by Saito[7–9] and Mishra,[10–12] proving the prominent effect of FPs. The low potential metal plate enables the redistribution of the E-field and the reduction of the peak field.[13–16] However, the frequency characteristic is unavoidably affected due to parasitics induced by the dielectric capacitance under the FP.[17] Meanwhile, depleting the two-dimensional electron gas (2DEG) density near the gate edge by low power fluorine (F^-) ions injection provides immobile negative charges in the AlGaN barrier and effectively depletes the electrons in the channel, which can modulate the fatal E-field peak with minimum parasitic. This method was first proposed by Song *et al.*[18] This low-density drain HEMT (LDD-HEMT) shows another method to enhance BV and reduce current collapse.[19,20]

In this paper, we proposed a novel AlGaN/GaN HEMT structure with a combination of small-size gate-FP and low-power LDD structure to effectively enhance the BV. Our experimental results indicated that the proposed LDD devices exhibit a three times enhancement of off-state BV.

2. Experiment

The AlGaN/GaN hetero structures were grown on a (0001) sapphire substrate in a metal organic chemical vapor deposition (MOCVD) system at Xidian University. The epitaxial layer contains a 20-nm undoped $Al_{0.30}Ga_{0.80}N$ barrier layer, a 1.2-nm AlN interlayer, a 1.6-μm unintentionally doped GaN buffer layer, and a low-temperature GaN nucleation layer. A sheet carrier density of 1.01×10^{13} cm^{-2}, an electron mobility of 1943 $cm^2/(V{\cdot}s)$, and a sheet resistance of 347 Ω/square of the hetero structures were measured using Hall effect measurements at room temperature.

The cross section of the LDD HEMT is shown in Fig. 1. The device fabrication commenced with mesa isolation using

*Project supported by the Key Program of the National Natural Science Foundation of China (Grant No. 61334002) and the Young Scientists Fund of the National Natural Science Foundation of China (Grant Nos. 61404100 and 61106106).

†Corresponding author. E-mail: xhma@xidian.edu.cn

© 2015 Chinese Physical Society and IOP Publishing Ltd

Cl_2/Ar plasma dry etching in a reactive ion etching (RIE) system, followed by the source/drain ohmic contacts, consisting of Ti/Al/Ni/Au annealed in N_2 ambient at 830 °C for 30 s. The resistance of the ohmic contact is 0.37 Ω·mm. Then a CF_4 plasma ion implantation with a RF source power of 100 W for 45 s was carried out in LDD area with different lengths of LDD (L_{LDD}), followed on with deposition of a 60-nm Si_3N_4 passivation layer at 300 °C by the plasma-enhanced chemical vapor deposition (PECVD) method. After that, a second CF_4 plasma treatment with a power of 120 W for 60 s was applied on the gate region and was subsequently annealed at 300 °C for 4 min to repair the plasma-induced damages. Finally, the Ni/Au/Ni Schottky gate and gate-FP was deposited by the e-beam evaporation method. Devices without LDD treatment or FP were also fabricated on the same wafer for a fair comparison. The fabricated devices have a gate–drain spacing (L_{GD}) of 2.5 μm, a gate-source spacing of 0.9 μm, a gate length of 0.5 μm, and a FP length (L_{FP}) of 0.5 μm, as shown in Fig. 1.

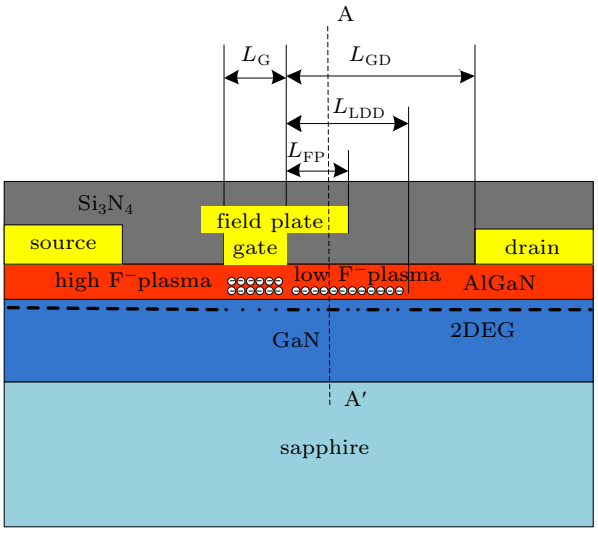


Fig. 1. (color online) Cross section of a FP HEMT with LDD treatment.

3. Results and discussion

The three-terminal off-state breakdown characteristics of the LDD MISHEMTs along with an ordinary T-gate HEMT are shown in Fig. 2. V_{GS} was set at −10 V to fully pinch off the devices. The breakdown measurement was carried out in air ambience. The limitation of the testing equipment is 200 V. The LDD spacing (L_{LDD}) is designed from 0 μm to 0.8 μm, the device with both FP and LDD (0.8 μm L_{LDD}, only 31% of the L_{GD}) achieves a BV enhancement up to two times compared with the device with only FP and three times compared with the device without FP or LDD. Although the best BV obtained was limited at 200 V, it was still far above other obtained BV in Refs. [17] and [18] with LDD treatment at almost the same gate to drain distance.

In Fig. 3(a) no obvious change in V_{th} and transconductance is observed because no F^- ions plasma is applied on the

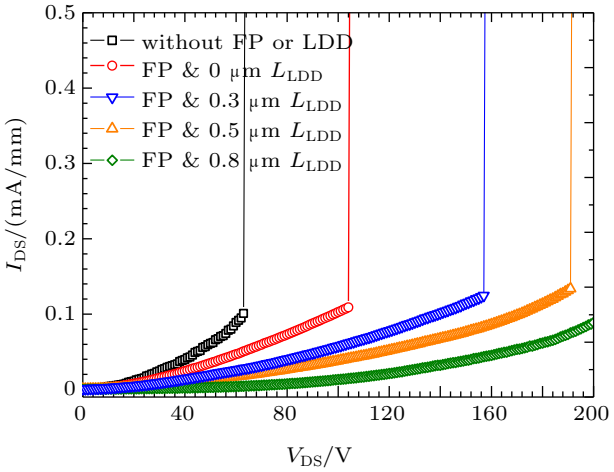


Fig. 2. (color online) Off-state BV in HEMTs with and without the LDD region and FP. The limitation of the testing equipment is 200 V.

gate region. So we believe that the LDD treatment has no influence on the transfer characteristic. The possible V_{th} shift can be considered as the F^- ion concentration changing under the gate as a result of non-self-alignment between the two separate (the gate and the LDD) CF_4 plasma treatments. In Fig. 3(b), the output current shows slight degradation caused by the immobile negative fluorine charges reducing the 2DEG density and less than a 1 V increase of V_{knee} is observed. In Fig. 3(c) no obvious change of gate leakage current is observed, showing that the low-power F-injection in LDD has no influence on the leakage path deep in the GaN buffer.

To support the above analysis, two-dimensional device simulations on GaN HEMTs using Silvaco ATLAS were also performed. The physical structure of the simulated HEMT consisted of a 20-nm AlGaN barrier layer, a 0.2-μm GaN layer, a 0.5-μm gate length, and a 0.5-μm FP length, which exactly corresponds to the real geometric structure of the fabricated devices. The 2DEG areal density of 1.01×10^{13} cm^{-2} was chosen to fit the experimental curves in Fig. 4. Meanwhile, in order to take the CF_4 plasma treatment into account, the 2DEG areal density was adjusted at 0.3×10^{13} cm^{-2} under the gate to give the correct threshold voltages, and 0.6×10^{13} cm^{-2} under the LDD area. The 2DEG mobility in the channel was set to 1943 $cm^2/(V \cdot s)$, which is exactly equal to the actual AlGaN/GaN hetero material. The gate work function was set to 5.23 eV, corresponding to the work function of Ni as the first layer of gate metal. The other material parameters were the same as those used in Ref. [21].

Figure 4 presents the measured transfer (I_{DS}–V_{GS}) and output (I_{DS}–V_{DS}) characteristics along with simulation curves for AlGaN/GaN HEMTs with both 0 μm and 0.8 μm L_{LDD}. The simulation curves are in accord with the experimental results. After that, by using this well-fitted device structure, we preformed simulation of E-field distribution of the LDD devices at V_{DS} of 150 V and V_{GS} of −6 V, as shown in Fig. 5. The normal device without LDD and FP shows its electric field peak up to 4 MV/cm, which is beyond the GaN limit, so the

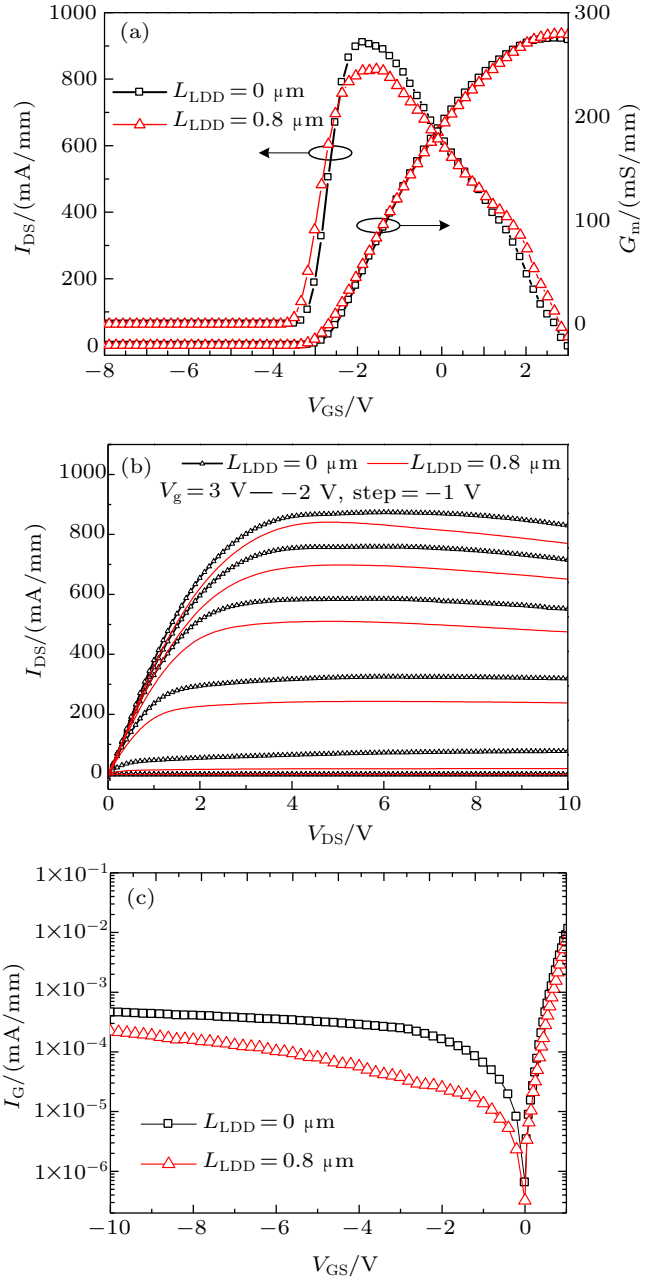


Fig. 3. (color online) Comparison of (a) dc transfer, $V_{ds} = 6$ V, (b) output characteristics, and (c) I_G–V_{GS} characteristics between devices with and without the LDD treatment.

actual BV of this device must be below 150 V. Meanwhile, the simulated electric field peak of LDD-HEMT is effectively reduced, revealing the reason for the BV enhancement in the experimental results. It is known that FP can efficiently ease the E-field peak near the gate edge by changing it into two lower peaks (the other is near the FP edge). The LDD further modulates the E-field into three peaks (the third is near the LDD edge) with an even lower concentration value. The device with both FP and 1.0-μm LDD showed the lowest electric field peak. Thus, the device with both FP and LDD is the least likely to reach the critical E-field of GaN material and achieved the highest BV.

According to Ref. [22], F^- ions as negatively immobile charges cause an upward bending of the conduction band and lead to an increase in Schottky barrier height. The simulated conduction band energy of the AlGaN/GaN hetero structures along the cross section of AA′ in Fig. 1 is shown in Fig. 6. This proves that the LDD treatment raised the conduction band energy. This enhanced band energy depletes the channel electrons and causes a relieved E-field density in the LDD area.

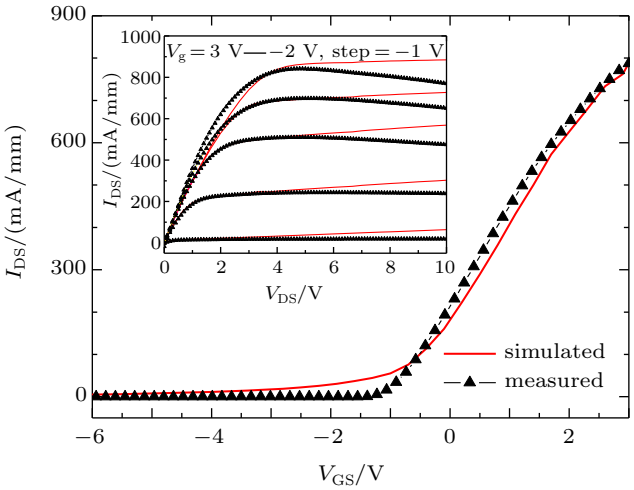


Fig. 4. (color online) Electric field distribution in the LDD & FP structure as a function of the LDD spacing.

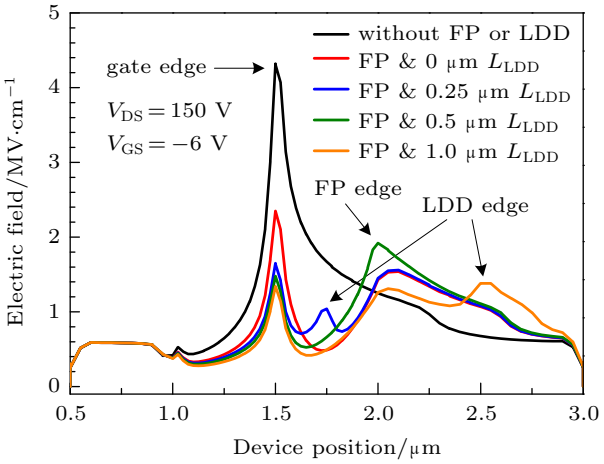


Fig. 5. (color online) Electric field distribution in the LDD & FP structure as a function of the LDD spacing.

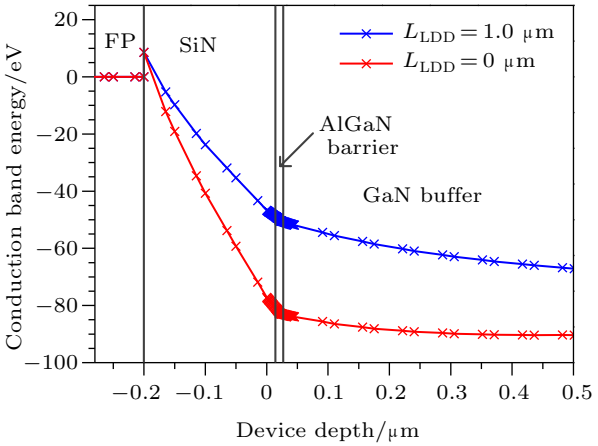


Fig. 6. (color online) Conduction band energy at V_{DS} of 150 V and V_{GS} of −6 V along the cross section of AA′ in Fig. 1.

4. Conclusion

By using both the field plate and the F^- ions injection in the LDD area, we have demonstrated an AlGaN/GaN HEMT with modified off-state breakdown behaviors. The obvious effect of BV enhancement was achieved without device degradation. The BV is far above other works with LDD treatment, in spite of testing equipment limitation. By using two-dimensional device simulations, the mechanism of the LDD treatment was supposed to be an enhanced band energy and depleted channel electrons in the LDD area, leading to modified E-field distribution and increased BV of the device.

References

[1] Pengelly R S, Wood S M, Milligan J W, Sheppard S T and Pribble W L 2012 *IEEE Trans. Microw. Theory Technol.* **60** 1764

[2] Milligan J W, Sheppard S T, Pribble W, Wu Y, Muller S and Palmour J W 2007 *IEEE Radar Conference*, April 17–20, 2007, Boston, MA, USA, pp. 960–964

[3] Yue Y Z, Hu Z Y, Guo J, Rodriguez B S, Li G W, Wang R H, Faria F, Fang T, Song B, Gao X, Guo S, Kosel T, Snider G, Fay P, Jena D and Xing H L 2012 *IEEE Electron Device Lett.* **33** 988

[4] Ostermaier C, Pozzovivo G, Carlin J F, Basnar B, Schrenk W, Douvry Y, Gaquière C, DeJaeger J C, Cico K, Fröhlich K, Gonschorek M, Grandjean N, Strasser G, Pogany D and Kuzmik J 2009 *IEEE Electron Device Lett.* **30** 1030

[5] Wang R, Li G W, Laboutin O, Cao Y, Johnson W, Snider G, Fay P, Jena D and Xing H L 2011 *IEEE Electron Device Lett.* **32** 892

[6] Cai Y, Zhou Y G, Lau K M and Chen K J 2006 *IEEE Trans. Electron Devices* **53** 2207

[7] Saito W, Nitta T, Kakiuchi Y, Saito Y, Tsuda K, Omura I and Yamaguchi M 2007 *IEEE Electron Device Lett.* **28** 676

[8] Saito W, Nitta T, Kakiuchi Y, Saito Y, Tsuda K, Omura I and Yamaguchi M 2007 *IEEE Trans. Electron Devices* **54** 1825

[9] Saito W, Nitta T, Kakiuchi Y, Nitta T, Saito Y, Noda T, Fujimoto H, Yoshioka A, Ohno T and Yamaguchi M 2010 *IEEE Electron Device Lett.* **31** 659

[10] Xing H L, Dora Y, Chini A, Heikman S, Keller S and Mishra U K 2004 *IEEE Electron Device Lett.* **25** 161

[11] Dora Y, Chakraborty A, McCarthy L, Keller S, DenBaars S P and Mishra U K 2006 *IEEE Electron Device Lett.* **27** 713

[12] Kolluri S, Pei Y, Keller S, Denbaars S P and Mishra Y K 2009 *IEEE Electron Device Lett.* **30** 584

[13] Bahat-Treidel E, Hilt O, Brunner F, Sidorov V, Würfl J and Tränkle G 2010 *IEEE Trans. Electron Devices* **57** 1208

[14] Xie G, Xu E, Lee J M, Hashemi N, Zhang B, Fu F Y and Wai T N 2012 *IEEE Electron Device Lett.* **33** 670

[15] Zhao S L, Mi M H, Hou B, Luo J, Wang Y, Dai Y, Zhang J C, Ma X H and Hao Y 2014 *Chin. Phys. B* **23** 107303

[16] Zhang K, Cao M Y, Lei X Y, Zhao S L, Yang L Y, Zheng X F, Ma X H and Hao Y 2013 *Chin. Phys. B* **22** 097303

[17] Brannick A, Zakhleniuk N A, Ridley B K, Shealy J R, Schaff W J and Eastman L F 2009 *IEEE Electron Device Lett.* **30** 436

[18] Song D, Liu J, Cheng Z Q, Tang W, Lau K M and Chen K J 2007 *Proceedings of the 19th International Symposium on Power Semiconductor Devices and ICs*, May 27–30, 2007, Jeju, Korea, pp. 257–260

[19] Suita M, Nanjo T, Oishi T, Abe Y and Tokuda Y 2008 *Electron. Lett.* **44** 1378

[20] Wang M J and Chen K J 2011 *IEEE Trans. Electron Devices* **58** 460

[21] *ATLAS User's Manual, SILVACO Int., Santa Clara*, CA, 2010

[22] Cai Y, Zhou Y G, Lau K M and Chen K J 2006 *IEEE Trans. Electron Devices* **53** 2207